the ASME, Series E, Journal of Applied Mechanics, Vol. 35, Dec. 1968, pp. 625–630.

[2] Goldstein, S., "Concerning Some Solutions of the Boundary Layer Equations in Hydrodynamics," *Proceedings of the Cambridge Philosophical Society*, Vol. XXVI, 1930, pp. 1–30.

[3] Lykoudis, P., "A Review of Hypersonic Wake Studies," May 1965, RM-4493-ARPA, The Rand Corp., Santa Monica, Calif.

[4] Van Dyke, M., "A Survey of Higher-Order Boundary Layer Theory," SUDAER, No. 326, 1967, Department of Aeronautics and Astronautics, Stanford University, Palo Alto, Calif.

[5] Dennis, S. C. R. and Dunwoody, J., "The Steady Flow of a Viscous Fluid Past a Plate," *Journal of Fluid Mechanics*, Vol. 24, March 1966, pp. 577–595.

[6] Imai, I., "On the Viscous Flow Near the Trailing Edge of a Flat Plate," *Proceedings of the XIth International Congress of Applied Mechanics*, Munich, 1964, pp. 663–671.

[7] Cheng, R. T., *An Investigation of the Laminar Flow Around the Trailing Edge of a Flat Plate*, Ph.D. dissertation, 1967, University of California, Berkeley, Calif.

[8] Imai, I., "A New Approximation for the Viscous Flow Near the Trailing Edge of a Flat Plate," presented at the 12th International Congress of Applied Mechanics, Stanford University, Aug. 26–31, 1968.

[9] Goldburg, A. and Cheng, S. I., "The Anomaly in the Application of PLK and Parabolic Coordinates to the Trailing Edge Boundary Layer," *Journal of Mathematics and Mechanics*, Vol. 10, 1961, p. 529.

[10] Carrier, G. F. and Lin, C. C., "On the Nature of the Boundary Layer Near the Leading Edge of a Flat Plate," *Quarterly of Applied Mathematics*, Vol. III, 1948, pp. 63–68.

[11] Lugt, H. J. and Schwiderski, E. W., "Flow Around Dihedral Angles," *Proceedings of the Royal Society*, Vol. A285, May 1965, p. 382.

[12] Weinbaum, S., "On the Singular Points in the Laminar Two-Dimensional Near Wake Flow Field," *Journal of Fluid Mechanics*, Vol. 33, 1968, pp. 38–63.

[13] Stewartson, K., "On the Flow Near the Trailing Edge of a Flat Plate," *Proceedings of the Royal Society*, Vol. A306, 1968, pp. 275–290.

[14] Stewartson, K., "On the Flow Near the Trailing Edge of a Flat Plate II," *Mathematika*, Vol. 16, Pt. 1, June 1969, pp. 106–121.

[15] Messiter, A. F., "Boundary Layer Flow Near the Trailing Edge of a Flat Plate," *SIAM Journal of Applied Mathematics*, Vol. 18, Jan. 1970, pp. 241–257.

[16] Talke, F. E. and Berger, S. A., "The Flat Plate Trailing Edge Problem," *Journal of Fluid Mechanics*, Vol. 40, Pt. 1, Jan. 1970, pp. 161–190.

[17] Van Dyke, M., "A Method of Series Truncation Applied to Some Problems in Fluid Mechanics," SUDAER No. 247, Department of Aeronautics and Astronautics, Stanford University, 1965.

[18] Giesing, J. P., "Extension of the Douglas Neumann Program to Problems of Lifting Infinite Cascades," LB 31653, July 1964, Douglas Aircraft Company, Los Angeles, Calif.

[19] Schneider, L. I., "Alternating Difference Implicit Techniques for Solution of LaPlace and Poisson Equation on Two Dimensions," TFD 68-129, June 1968, North American Rockwell Corporation, Los Angeles, Calif.

[20] Peaceman, D. W. and Rachford, H. H., "The Numerical Solution of Parabolic and Elliptic Differential Equations," *SIAM Journal*, Vol. 3, 1955, pp. 28–41.

[21] Schneider, L. I., "The Evolution of the Laminar Wake and Its Upstream Influence," Ph.D. dissertation, 1969, University of California, Los Angeles, Calif..

APRIL 1971 AIAA JOURNAL VOL. 9, NO. 4

An Approach to the Dust Devil Vortex

SAMUEL E. LOGAN*
California Institute of Technology, Pasadena, Calif.

A simple analytical model is developed for prescribing the velocity fields in a dust devil, a small intense vortex phenomenon common in arid regions. Since observations by Sinclair indicate that the tangential motion resembles a Rankine combined vortex with superimposed radial inflow near the ground, the model proposed has an "outer" inviscid region of cyclostrophic balance and an "inner" inflow region controlled by viscosity. A perturbation analysis is first performed showing the tangential and radial boundary layer velocity profiles to have the well-known oscillatory nature of the Ekman and Bödewadt solutions. A momentum integral method using these velocity profiles as trial functions is then employed to obtain the functional dependences of the boundary-layer thickness and the integrated radial and vertical mass flows. These are found to depend on the square root of the nondimensional eddy viscosity or inverse Reynolds number of the outer flow, and compare favorably with the measurements of Sinclair.

Nomenclature

a^* = parameter in Burger's vortex solution.
$A(r)$ = amplitude coefficient of radial velocity, perturbation solution
B,D,F,I_1 = velocity profile constants, integral solution
$E(r)$ = amplitude coefficient of radial velocity, integral solution
f,g = radial, tangential trial functions, integral solution
$M(r)$ = integrated inward radial mass flow in boundary layer
p = $p^*/\rho_0^* V_m^{*2}$, dimensionless pressure
p_a^* = ambient pressure
r = r^*/r_m^*, dimensionless radius
r_m^* = dimensional radius of maximum tangential velocity V_m^*
R_0 = $V_m^*/(2\Omega_z^* r_m^*)$, the Rossby number
u_{max} = maximum radial velocity at a given radius
(u,v,w) = $(u^*/V_m^*,\ v^*/V_m^*,\ w^*/V_m^*)$ dimensionless radial, tangential, vertical velocity components
V_m^* = maximum tangential velocity of outer vortex
$W(r)$ = vertical velocity above boundary layer, integral solution
z = z^*/r_m^*, dimensionless vertical coordinate
$\bar{z}$ = stretched vertical coordinate in boundary layer
$\beta(r)$ = $\delta(r)^4 v_0(r)^{8/3}$
$\Gamma_0(r)$ = $v_0 r$, dimensionless circulation of outer flow

Received October 29, 1969; revision received August 12, 1970. This work is based on the paper which won first place in the graduate division at the AIAA National Student Conference, October 1969.[1] The author wishes to thank H. W. Ellsaesser for his suggestion of the problem and initial guidance.

* Graduate Student in Aeronautics, Karman Laboratory of Fluid Mechanics; Fannie and John Hertz Foundation Fellow. Student Member AIAA.

$\delta(r)$ = $\delta(r)^*/r_m^*$, dimensionless boundary-layer thickness
ϵ^* = dimensional eddy viscosity
ϵ = $\epsilon^*/V_m^* r_m^*$, dimensionless eddy viscosity or inverse Reynolds' number of outer flow
η = z/δ, boundary-layer coordinate
$\varkappa$ = vertical velocity scaling factor, perturbation analysis
$\xi(r)$ = $[2v_0/r(v_0/r + \partial v_0/\partial r)]$
ν = viscosity coefficient in Burger's vortex solution
ρ = density
$2\Omega_z^*$ = vertical component of Coriolis parameter

Subscripts

0 = external flow variable
1 = boundary-layer flow variable, perturbation analysis

Superscript

* = dimensional quantities

I. Introduction

ATMOSPHERIC thermals, vertical convective currents whose existence and initiation depend primarily on buoyancy, have for many years been of great scientific interest to meteorologists as well as of use to sailplane enthusiasts. A very interesting special case of atmospheric thermal is the dust devil, an intense vortex phenomenon found in arid regions where a thin thermal boundary layer with a highly super-adiabatic lapse rate develops due to solar surface heating.† Ives[3] reports that the lapse rate at the ground can exceed 2000 times the adiabatic value as in Fig. 1. Since an adiabatic lapse rate defines neutral static stability, such a thermal layer represents a large source of potential energy. This potential energy source and some initial vorticity are generally agreed to be the dominant factors in the formation of dust devils. Once started, the vortex is maintained by the inflow of fresh surface-heated environmental air (the fuel) toward the center (core) where buoyancy forces carry it aloft. The intense rotary motion is generated and sustained by the tendency of the air to conserve its angular momentum as it spirals toward the center. The rotation and the updraft result in a helical motion, often made visible by entrained surface dust and debris which is carried aloft.

These dust columns vary in height from a few feet to nearly 2000 ft but thermal currents above the vortex can persist to heights greater than 15,000 ft according to Sinclair's sailplane measurements.[4] Dust devil lifetimes vary from a few sec to nearly 20 min, most lasting under 2 min.[5] Ives observed an exceptional example during construction of a large railroad embankment near Sonora which removed approximately 1 yd³ of sand per hour for 4 hr and was eventually broken up by moving a bulldozer into the vortex.[3] Dust devils depend directly on the availability of heated boundary-layer air and dissipate quickly if this fuel is removed.

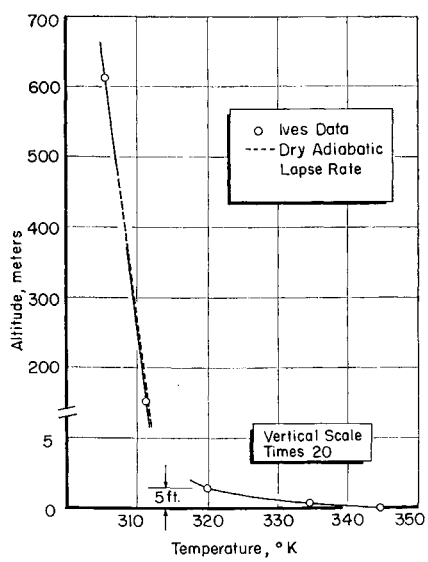

Fig. 1 Environmental temperature distribution favorable for dust devil formation, from Ives.

† Michelson[2] has shown that a shear flow can provide a stabilizing influence to allow the formation of such a layer with a density inversion.

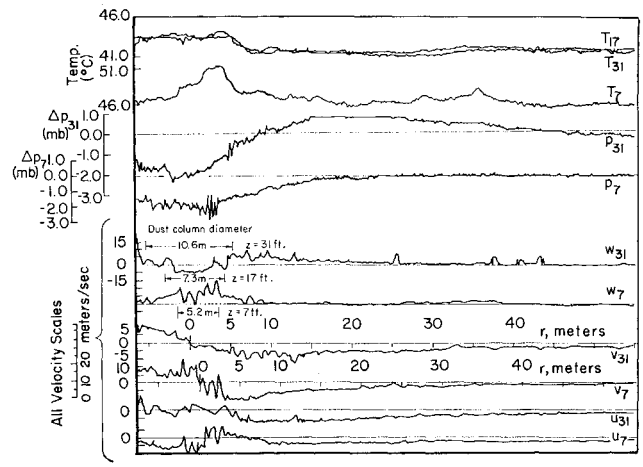

Fig. 2 Sinclair's dust devil measurements.

The dust columns tend to meander across the desert floor at the prevailing wind speed. However, Sinclair[5] has observed an apparent critical wind speed above which dust devil activity decreases, probably because of destruction of the heated boundary layer by increased vertical mixing and shearing of the vortices near the ground.

The vertical velocities near the ground can at times be appreciable and exceed 25 mph. In an amusing account Ives relates estimating these vertical currents by measuring the terminal velocities of small animals sometimes lifted by dust devils.[3]

To date, the most detailed measurements of dust devil velocity, pressure, and temperature fields have been made by Sinclair.[4,5] A typical set of his measurements, taken at altitudes of 7 and 31 ft, is reproduced in Fig. 2. He measured tangential velocities approaching 15 m/sec, vertical velocities of 10 m/sec (at 7 ft altitude) and maximum radial velocities of about 5 m/sec. Commonly, between the environment and the core there is a pressure drop in excess of 2 mb and a temperature increase of 4°C or more.

As shown by Sinclair in Fig. 3, near the center the tangential flow closely approximates solid body rotation whereas at larger distances it resembles a free vortex. (Figs. 2 and 3 are the same dust devil.)

Rotating flows have been treated by many workers including Taylor, Von Karman, and Batchelor, and a comprehensive review exists in Greenspan.[6] Kuo[7] has done extensive work on hurricanes and large-scale convective vortices while others such as Barcilon[8] and Maxworthy[9,10] have addressed themselves to dust devils and laboratory vortex phenomena. An excellent (although somewhat qualitative) review of geophysical vortices in general is given by Morton.[11]

The present analysis is a simple approach to the dust devil vortex in two parts. The first is a perturbation analysis demonstrating that the tangential and radial boundary-layer velocity profiles have oscillatory form, as also shown by Kuo.[7] However, as the perturbation solution cannot adequately describe the flow outside the radius of maximum tangential velocity, an integral method proposed by Mack[12] is applied. Using velocity profiles from the first section, the functional dependences of the boundary-layer thickness and the integrated radial and vertical mass flows are obtained and found

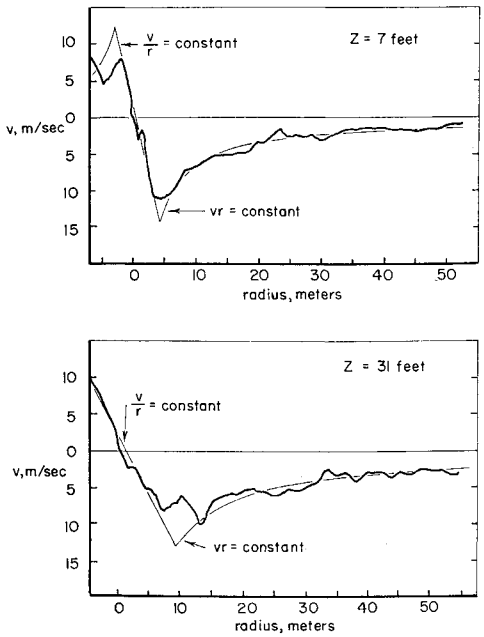

Fig. 3 Observed radial distribution of the mean tangential velocity at two altitudes z = 7 and 31 ft.

to depend on the square root of the nondimensional eddy viscosity or inverse Reynolds number of the outer flow. With proper choice of this eddy viscosity, reasonable qualitative and quantitative agreement is found with the measurements of Sinclair.

II. Boundary-Layer Velocity Profiles

The equations for steady, incompressible flow are

$$\nabla\cdot\mathbf{v}^* = 0 \tag{1}$$

$$(\mathbf{v}^*\cdot\nabla)\mathbf{v}^* + 2\Omega_z \times \mathbf{v}^* = -(1/\rho^*)\nabla p^* + \epsilon^*\nabla^2\mathbf{v}^* \tag{2}$$

where $\mathbf{v}^* = (u^*, v^*, w^*)$, and the asterisks refer to dimensional quantities.

The basic boundary-layer velocity profiles can be exhibited by balancing the dominant terms in the equation of motion. The major assumptions are as follows. a) For dust devil scales, the Coriolis acceleration term is negligible compared to the centrifugal acceleration.‡ b) Above the boundary layer, friction is negligible, the centrifugal force due to fluid rotation balances the radial pressure gradient, and the radial velocity is zero. c) In the boundary layer the radial pressure gradient is constant§ and exceeds the local centrifugal force causing radial mass inflow, which in turn by mass continuity forces a vertical velocity through the top of the layer. d) The leading dissipation term in the boundary layer is $\epsilon^*\partial^2/\partial z^{*2}$.¶

Using these assumptions, assuming axisymmetry, and nondimensionalizing with respect to V_m^*, the maximum tangential velocity in the outer flow, and r_m^*, the radius of maximum tangential velocity, gives

$$(1/r)[\partial(ru)/\partial r] + (\partial w/\partial z) = 0 \tag{3}$$

$$u(\partial v/\partial r) + w(\partial v/\partial z) + (uv/r) = \epsilon(\partial^2 v/\partial z^2) \tag{4}$$

$$u(\partial u/\partial r) + w(\partial u/\partial z) - (v^2/r) = -(1/\rho)(\partial p/\partial r) + \epsilon(\partial^2 u/\partial z^2) \tag{5}$$

where $\epsilon = \epsilon^*/V_m r_m$ is a nondimensional eddy viscosity, or inverse Reynolds number of the outer flow.

Assuming the outer flow variables, denoted $(\ )_0$, depend only on r and the inner boundary-layer flow variables $(\ )_1$ depend on both r and z, we write

$$\begin{aligned} v(r,z) &= v_0(r) - v_1(r,z) \\ u(r,z) &= u_1(r,z) \\ w(r,z) &= \varkappa[w_0(r) - w_1(r,z)] \end{aligned} \tag{6}$$

where $\varkappa$ = constant = o(1), to be determined.

Boundary conditions are

$$\begin{aligned} v_1(r,\infty) = u_1(r,\infty) = w_1(r,\infty) = 0 \\ w_1(r,0) = w_0(r) \quad v_1(r,0) = v_0(r) \end{aligned} \tag{7}$$

Plugging Eq. (6) into Eqs. (4) and (5) gives for the outer flow above the boundary layer ($\epsilon \to 0$)

$$v_0^2/r = (1/\rho)(\partial p/\partial r) \text{(cyclostrophic balance)} \tag{8}$$

To linearize Eqs. (4) and (5) we employ the additional assumptions that the terms in w are smaller order, $O(w\partial v/\partial z) < O(u\partial v/\partial r)$ etc., and $O(v_1) < O(v_0)$, since the region where $O(v_1) = O(v_0)$ is confined to a very thin region near the ground relative to the total boundary-layer thickness. With these, the boundary-layer equations become

$$u_1(\partial v_0/\partial r) + u_1(v_0/r) = -\epsilon(\partial^2 v_1/\partial z^2) \tag{9}$$

$$(2v_0/r)v_1 = \epsilon(\partial^2 u_1/\partial z^2) \tag{10}$$

which can be combined to yield

$$(\xi^4\epsilon^2)(\partial^2 v_1/\partial z^4) + v_1 = 0 \tag{11}$$

where $\xi(r) = \{2v_0(r)/r[v_0(r)/r + \partial v_0/\partial r]\}^{-1/4}$. Stretching the vertical scale introducing $z = (2)^{1/2}\xi(r)\epsilon^{1/2}\bar{z}$, then

$$(\partial^4 v_1/\partial\bar{z}^4) + 4v_1 = 0$$

and (12)

$$\partial^4 u_1/\partial\bar{z}^4 + 4u_1 = 0$$

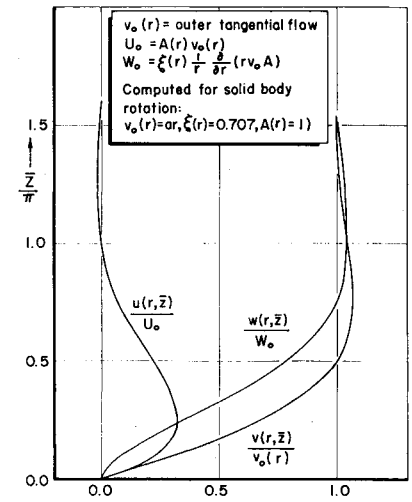

Fig. 4 Boundary-layer velocity profiles at fixed radius from perturbation analysis.

‡ Typically $10^{-4} < (\Omega_z^* v^*)/(v^{*2}/r^*) < 10^{-2}$. This has the important implication that, unlike large-scale atmospheric motions such as hurricanes, the dust devil has no preferred direction of rotation, a fact experimentally verified by Sinclair.[4] This ratio is essentially an inverse "Rossby number," $R_0 = V_m^*/2\Omega_z^* r_m^*$, which is large for the dust devil.

§ Maxworthy[10] argues that since the vertical flow imposed on the boundary layer can be considerable, $\partial p^*/\partial z^*$ may be no longer negligible. However, Sinclair's measurements in Fig. 2 indicate that $\partial p^*/\partial z^*$ is generally small compared to $\partial p^*/\partial r^*$, which is nearly identical at 7- and 31-ft altitude.

¶ Sinclair's measurements in Fig. 2 indicate there are significant velocities at 7-ft altitude which must decrease to zero at the ground. Since the radial scale of variation is at least several times this, neglect of $\nu\partial^2/\partial r^2$ etc., is justified near the ground (but not in a vortex in free space as considered by Long[13]).

which have solutions, using Eqs. (6) and (7)

$$v(r,z) = v_0(r)[1 - \cos\bar{z}e^{-\bar{z}}]$$
$$u(r,z) = v_0(r)A(r)\sin\bar{z}e^{-\bar{z}} \quad (13)$$

where $A(r) = [2v_0/(v_0 + r\partial v_0/\partial r)]^{1/2}$. The vertical velocity is found from Eq. (3)

$$(1/r)[\partial(ru)/\partial r] + (\varkappa/\xi\epsilon^{1/2})(\partial w_1/\partial\bar{z}) = 0 \quad (14)$$

To preserve the structure of the continuity equation we require $(\varkappa/\xi\epsilon^{1/2}) = 1$, or choose $\varkappa = \xi(r)\epsilon^{1/2} = o(1)$. Integrating Eq. (14) gives

$$w(r,z) = \xi(r)\epsilon^{1/2}\{(1/r)[\partial(rv_0A)/\partial r][1 - 2\sin(\bar{z} + \pi/4)e^{-\bar{z}}] + (2/\epsilon)^{1/2}v_0A(\partial/\partial r)[1/\xi(r)]\sin\bar{z}e^{-\bar{z}}\} \quad (15)$$

The boundary-layer thickness $h(r)$ is defined as the height at which $u(r,z)$ first becomes zero, or

$$h(r) = 2^{1/2}\pi\epsilon^{1/2}\xi(r)$$

The behavior of the three velocity components for fixed radius is shown in Fig. 4. The oscillatory nature is characteristic of Ekman (linear) solutions and Bödewadt (nonlinear) solutions. Kuo has obtained similar profiles for the boundary layer of a convective atmospheric vortex.[7] For the special case of solid body rotation $\xi(r) \equiv 2^{-1/2}$ and $A(r) = 1$, and the result checks with a result by Cole[14] using matched asymptotic expansions.

However, as also pointed out by Kuo, the present first-order perturbation solution does not correctly describe the flow far beyond the point of maximum tangential velocity. [For Burger's solution for v_0, Fig. 5, $\xi(r)$ grows exponentially at large r]. However, using profiles of form (13) in an established integral method should yield reasonable distributions of integrated quantities.

III. Application of the Integral Method

Mack[12] shows that a simplified momentum integral method using the integrated tangential momentum equation and a radial "compatibility condition" adequately describes the laminar boundary layer on a finite disk in a rotating flow. A similar approach should yield a good description for the turbulent boundary layer in the dust devil if an eddy viscosity ϵ is used and profiles of the form (13) found in the previous section are applied. If the boundary layer thickness is $\delta(r)$, integration of Eq. (3) across the layer and using $u(r,z = \delta) = 0$ gives

$$W(r) = -\frac{1}{r}\frac{d}{dr}\int_0^{\delta(r)}(ru)dz \quad (16)$$

for the vertical velocity distribution in the outer flow. Defining the total inward radial mass flow as

$$M(r) = -2\pi r\int_0^{\delta(r)}udz \quad (17)$$

gives

$$W(r) = (1/2\pi r)(dM/dr) \quad (18)$$

Integrating Eq. (4) using Eqs. (3) and (16) yields the integrated tangential momentum equation

$$\frac{d}{dr}\left(r^2\int_0^{\delta}uv\,dz\right) - v_0r\frac{d}{dr}\left(r\int_0^{\delta}udz\right) = -r^2\epsilon\left.\frac{\partial v}{\partial z}\right|_{z=0} \quad (19)$$

Tangential and radial velocity profiles are assumed to be formally

$$v(r,z) = v_0(r)g(\eta) \quad (20)$$
$$u(r,z) = v_0(r)E(r)f(\eta) \quad (21)$$

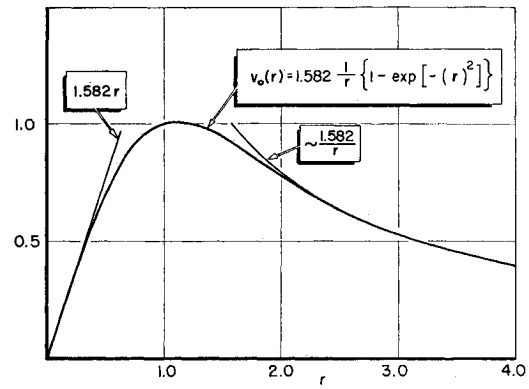

Fig. 5 Burgers' vortex outer flow distribution.

where $\eta = z/\delta$. Evaluation of the radial momentum equation (5) at $z = 0$ and using Eq. (8) requires

$$\epsilon(\partial^2u/\partial z^2)_{z=0} = v_0(r)^2/r$$

a radial compatability condition, from which

$$E(r) = [v_0(r)/r][\delta(r)^2/\epsilon f''(0)] \quad (22)$$

and the radial velocity is

$$u(r,z) = [v_0(r)^2/r][\delta(r)^2/\epsilon][f(\eta)/f''(0)] \quad (23)$$

By substitution of Eqs. (23) and (20) into Eq. (19) and after considerable manipulation, Mack shows the momentum equation (19) can be written in the form

$$\frac{d\beta}{dr} - \left[\frac{4}{3}(1 - B)\frac{d}{dr}(\log rv_0)\right]\beta - \left\{rv_0^{2/3}\left[\frac{4}{3}\epsilon^2f''(0)D\right]\right\} = 0 \quad (24)$$

where $\beta = \delta^4v_0^{8/3}$ and B and D are velocity profile constants

$$B = \int_0^1 f(1 - 2g)d\eta \Big/ \int_0^1 f(1 - g)d\eta$$
$$D = g'(0) \Big/ \int_0^1 f(1 - g)d\eta \quad (25)$$

Introducing $\Gamma_0(r) = v_0(r)r$ as the dimensionless circulation of the outer flow and integrating Eq. (24) gives

$$\delta^4(r) = \delta^4(R)\left(\frac{r}{R}\right)^{8/3}\left[\frac{\Gamma_0(R)}{\Gamma_0(r)}\right]^{4/3(3-B)} + \left[-\frac{4}{3}\epsilon^2f''(0)D\right]\frac{r^{8/3}}{\Gamma_0(r)^{4/3(1+B)}}\int_r^R\frac{r^{1/3}dr}{\Gamma_0^{2/3(1-2B)}} \quad (26)$$

where the integration has been carried out to some $r = R$ at which the boundary-layer thickness is $\delta(R)$. For his finite disk, Mack takes $R = 1$ and assumes $\delta(1) = 0$, and is thus left with only the second term. For the dust devil we let R become large and assume $\delta(R)$ approaches zero and $\Gamma_0(R)$ a constant so that

$$\delta^4(r) = \left[-\frac{4}{3}\epsilon^2f''(0)D\right]\frac{r^{8/3}}{\Gamma_0(r)^{4/3(1+B)}}\int_r^R\frac{r^{1/3}dr}{\Gamma_0^{2/3(1-2B)}} \quad (27)$$

Evaluation of this integral yields $\delta(r)$ and hence the other integrated quantities $M(r)$ and $W(r)$. In particular, from Eq. (17) the integrated inwards radial mass flow is

$$M(r) = -\frac{2\pi}{f''(0)}v_0(r)^2\frac{\delta(r)^3}{\epsilon}\int_0^1f(\eta)d\eta \quad (28)$$

Since $\delta \sim \epsilon^{1/2}$, $M(r) \sim \epsilon^{1/2}$ and $W(r) \sim \epsilon^{1/2}$. However, the radial inflow velocity $u(r)$ given in Eq. (23) is seen to be independent of ϵ since $\delta^2 \sim \epsilon$.

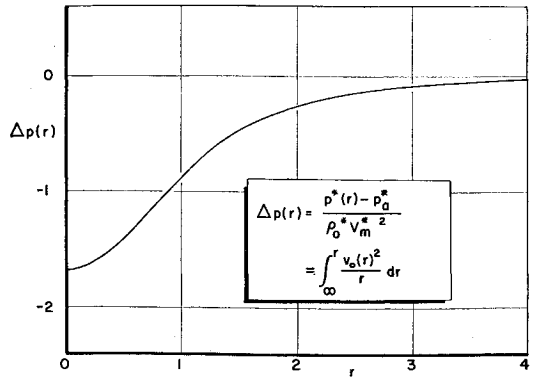

Fig. 6 Radial pressure distribution required to support Burgers' tangential velocity distribution.

IV. Trial Functions

A. Burgers' Vortex Outer Flow

Sinclair's measurements in Fig. 3 suggest that the outer flow $v_0(r)$ can be well modelled by Burger's vortex**

$$v_0(r) = (1/r)(1 - e^{-r^2})/(1 - e^{-1}) = (1.582/r)(1 - e^{-r^2})$$

or

$$\Gamma_0(r) = 1.582(1 - e^{-r^2}) \tag{29}$$

which closely approximates solid body rotation for small r and a free vortex for large r, as seen in Fig. 5. The radial pressure gradient required to support Burger's tangential velocity field according to Eq. (8) is shown in Fig. 6 and exhibits the basic shape of those measured by Sinclair, Fig. 2.

The dimensionless pressure drop $\Delta p(0)$ between the core and ambient pressure is 1.684 which corresponds to 1.9 mb for $\rho_0^* = 1.14$ kgm^{-3} and $V_m^* = 10$ msec^{-1}. Fig. 2 shows a measured pressure drop of 2 mb for V_m^* of 10 msec^{-1}.

B. Boundary-Layer Functions

Following Eq. (13) we choose

$$f(\eta) = \sin\pi\eta e^{-\pi\eta}$$
$$g(\eta) = 1 - \cos\pi\eta e^{-\pi\eta} \tag{30}$$

so that at $\eta = 1$, $u(r,1) = 0$. Then we have $f''(0) = -2\pi^2$,

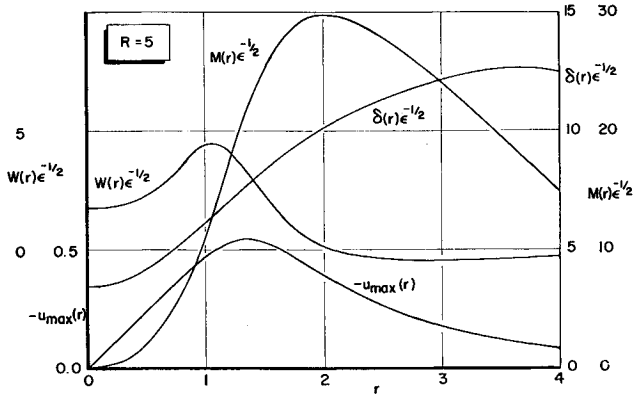

Fig. 7 Radial dependence of integral solution functions for $R = 5$.

** Burgers'[15] exact vortex solution to the Navier-Stokes equations has the tangential component $v^*(r^*) = (\Gamma^*/2\pi r^*)\,[1 - \exp(-a^* r^{*2}/2\nu^*)]$. We have introduced a dimensionless radius $r_m^* = (2\nu^*/a^*)^{1/2}$ and normalized so that $v(r = r^*/r_m^* = 1) = 1$. Kuo[7] has shown that the constant a^* is proportional to the atmospheric stability factor, typically 0.1–0.7 sec^{-1} for the dust devil.

Table 1 Values of dimensional eddy viscosity in literature

Investigator	ϵ^*, m^{2}sec^{-1}	Phenomenon
Sinclair[4]	5–15	Dust devil
Kuo[7]	1	Dust devil
Kuo[7]	5	Tornado
Long[13]	1–10	Dust devil, tornado
Rott and Lewellen[16]	10	Tornado
Gutman[17]	10	Water spout, tornado
Smith[18]	50	Hurricane

$g'(0) = \pi$ and the profile constants $B = -2.1807$ and $D = 79.105$. [Although these profiles result from an analysis which assumes the vertical velocity to be small, and thus are somewhat in error in the region of largest vertical velocities, application in Mack's momentum integral method should yield reliable results for the integrated quantities of total inward mass flow $M(r)$ and vertical velocity $W(r)$.]

V. Discussion of Results

A. Behavior near $r = 0$

Near the axis $r = 0$ the outer tangential flow closely approximates solid body rotation, $v_0(r) = ar$, as seen in Figs. 3 and 5. Assuming this to be true in a region $0 \le r \le r_s$ Eq. (27) can be written

$$\delta^4(r) = \left[-\frac{4}{3}\epsilon^2 f''(0)D\right]\frac{r^{-8B/3}}{a^{4/3(1+B)}}\left[a^{2/3(1-2B)}\int_r^{r_s} r^{(8B/3)-1}dr + \int_{r_s}^{R}\frac{r^{1/3}}{\Gamma_0^{2/3(1-2B)}}\,dr\right] = \left[-\frac{4}{3}\epsilon^2 f''(0)D\right]\left(-\frac{3}{8B}\right)\frac{1}{R^2}$$
$$\left\{1 - \left(\frac{r}{r_s}\right)^{-8B/3}\left[1 - \frac{8B}{3}a^2 fnc(R,r_s)\right]\right\}$$

Taking the limit $r \to 0$,

$$\delta^4(0) = [f''(0)D/2B](\epsilon^2/a^2) \tag{31}$$

since $B < 0$. Also $d(\delta^4)/dr = 0$ at $r = 0$. Using Eqs. (31), (28) and (18)

$$M(r < r_0) = 2\pi F^{1/4} I_1 \epsilon^{1/2} r^2$$

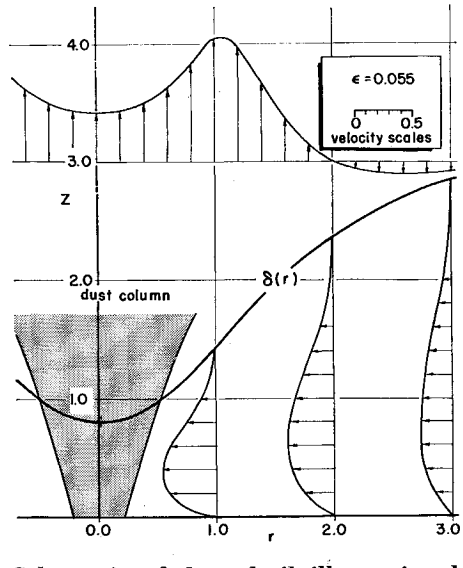

Fig. 8 Schematic of dust devil illustrating boundary layer, radial inflow, vertical velocity, and typical dust column size from Sinclair's measurements, Fig. 2. (Using $r_m^* = 10$ m and $\epsilon = 0.055$).

and

$$W(r < r_0) = 2F^{1/4}I_1\epsilon^{1/2}$$

near $r = 0$ where

$$F = [a^2/f''(0)](D/2B)^3$$

and

$$I_1 = \int_0^1 f(\eta)d\eta$$

It follows that $dM/dr = dW/dr = 0$ at $r = 0$ and from Eq. (23) it is seen that $u(r,z)$ is linear in r near the origin. Using functions (29) and (30), $\delta(0) = 3.46\,\epsilon^{1/2}$ and $W(0) = 1.745\,\epsilon^{1/2}$.

B. Behavior of Integral Solutions

Figure 7 shows the radial dependences of $\delta(r)\epsilon^{-1/2}$, $M(r)\epsilon^{-1/2}$ and $W(r)\epsilon^{1/2}$ for $R = 5$. Also shown is the maximum radial velocity at a given radius, u_{max}

$$u_{max} = [v_0^2(r)/r][\delta^2(r)/\epsilon]\{[f(\eta)]_{max}/f''(0)\}$$

which occurs at an altitude $\eta = \frac{1}{4}$ from Eq. (30) where $[f(\eta)]_{max} = 0.322$.

Comparison with the finite disk calculations of Mack[12] shows qualitative agreement for these functional dependences as would be expected. The vertical velocity has a maximum very near $r = 1$, the point of maximum tangential velocity, while u_{max} reaches a maximum near $r = 1.4$. The vertical velocity falls much faster with radius than does the radial velocity and beyond about $r = 2$ a weak downdraft exists as the total inward mass flow $M(r)$ begins to decrease. These results compare favorably with the measurements of Sinclair in Fig. 2. His vertical velocity measurement at 7 ft altitude shows such a weak downdraft starting at a radius of 10 m or approximately twice the radius of maximum tangential velocity at that altitude. Typical measured values of the inflow velocity, between 3–7 msec^{-1}, are consistent with the computed values of u_{max} between 0.3 and 0.5 for typical values of V_m^* of 10–15 msec^{-1}. However, the present analysis gives that the radii of maximum tangential and vertical velocities are nearly the same, whereas Sinclair notes that at times the radius of maximum vertical velocity is less.

C. Numerical Comparison with Observations

To fix the numerical value of the vertical velocity and the boundary-layer thickness, ϵ must be determined, which involves choosing a value for the (dimensional) eddy viscosity ϵ^*. Table 1 lists various values presented in the literature for ϵ^*. A choice of 1 to 15 m^{2}sec^{-1} appears reasonable for the dust devil. For $V_m^* = 10$ msec^{-1} and $r_m^* = 10$ m, $\epsilon^* = 1$ m^{2}sec^{-1} gives $\epsilon = 0.01$ and $W^*_{max} = 4.4$ msec^{-1}, while $\epsilon^* = 15$ m^{2}sec^{-1} gives $\epsilon = 0.15$ and $W^*_{max} = 17.1$ msec^{-1} since $W_{max} = 4.42$. Fig. 2 shows maximum vertical velocities near 10 msec^{-1} which would indicate an ϵ^* close to 5.5 m^{2}sec^{-1}. This comparison leaves little question that "eddy viscosity" is involved. A schematic of the dust devil is given in Fig. 8 illustrating the boundary-layer, radial and vertical velocities and a typical dust column size (from Fig. 2 using $r_m^* = 10$ m). For reference, 31 ft altitude would be close to $z = 1$ for $r_m^* = 10$ m. At the dust devil center, the boundary layer is 8 m deep and rapidly increases at larger r.

VI. Conclusions and Additional Discussion

It has been demonstrated that a simple momentum-integral method can adequately describe the gross features of a small atmospheric vortex such as the dust devil, and compare favorably with measurements. However, there are many very interesting aspects of such small vortices which have not been attempted such as subsidence within the core and "vortex breakdown." The former has been a question of much interest for many years, and proper analytical treatment should include the energy equation and buoyancy assuming this descending air to be cooler than that rising about it. In some cases Sinclair appears to have noticed such a phenomenon. This might have the additional implication of Smith's "radial stagnation point"[18] and perhaps require a complicated axial boundary layer along the lines of Barcilon,[8] with radial stress terms no longer ignored. Vortex breakdown has been observed by Maxworthy[10] in the laboratory to occur near the top of the boundary layer for intense sink vortices, and a similar phenomenon has been observed in tornadoes and very energetic dust devils.[10]

As a result of such unique and intriguing features, vortex phenomena remain of great practical and scientific interest, especially the many geophysical vortices occurring in nature.

References

[1] Logan, S. E., "A Simple Analytical Model for the Dust Devil," AIAA 19th Annual Region IV Student Conference at California State Polytechnic College, Pomona, California, May 1969; Rept. UCRL-50667, Lawrence Radiation Laboratory, Livermore, Calif.

[2] Michelson, I., "On Dust Devils," thesis, 1951, California Institute of Technology, Pasadena, Calif., pp. 1–34.

[3] Ives, R. L., "Behavior of the Dust Devil," *Bulletin of the American Meteorological Society*, Vol. 28, April 1947, pp. 168–174.

[4] Sinclair, P. C., "A Quantitative Analysis of the Dust Devil," thesis, 1966, University of Arizona, Tucson, Ariz.

[5] Sinclair, P. C., "General Characteristics of Dust Devils," *Journal of Applied Meteorology*, Vol. 8, Feb. 1969, pp. 32–45.

[6] Greenspan, H. P., *The Theory of Rotating Fluids*, Cambridge University Press, Great Britain, 1968.

[7] Kuo, H. L., "On the Dynamics of Convective Atmospheric Vortices," *Journal of the Atmospheric Sciences*, Vol. 23, Jan. 1966, pp. 25–42.

[8] Barcilon, A., "A Theoretical and Experimental Model for a Dust Devil," *Journal of the Atmospheric Sciences*, Vol. 24, Sept. 1967, pp. 453–466.

[9] Maxworthy, T., "The Flow Between a Rotating Disk and a Co-axial, Stationary Disk," Space Programs Summary 37–27, Vol. 4, Sec. 327, 1964, Jet Propulsion Laboratory, Pasadena, Calif.

[10] Maxworthy, T., "The Flow Creating a Concentration of Vorticity over a Stationary Plate," Space Programs Summary 37–44, Vol. 4, 1964, Jet Propulsion Laboratory, Pasadena, Calif., pp. 243–250; also private communications.

[11] Morton, B. R., "Geophysical Vortices," *Progress in Aeronautical Sciences*, Vol. 7, Pergamon Press, Oxford, 1966, pp. 145–194.

[12] Mack, L. M., "The Laminar Boundary Layer on a Disk of Finite Radius in a Rotating Flow. Part II: A Simplified Momentum Integral Method," Tech. Rept. 32–366, Jan. 1963, Jet Propulsion Laboratory, Pasadena, Calif.

[13] Long, R. R., "Vortex Motion in a Viscous Fluid," *Journal of Meteorology*, Vol. 15, Feb., 1958, pp. 108–112.

[14] Cole, J. D., "Viscous Boundary Layer in a Rotating Fluid," *Perturbation Methods in Applied Mathematics*, Blaisdell Publishing Co., Waltham Mass., 1968, pp. 176–181.

[15] Burgers, J. M., "A Mathematical Model Illustrating the Theory of Turbulence," *Advances in Applied Mathematics*, Vol. 1, Academic Press, N.Y., 1948, pp. 197–199.

[16] Rott, N. and Lewellen, W. S., "Boundary Layers and Their Interactions in Rotating Flows," *Progress in Aeronautical Sciences*, Vol. 7, Pergamon Press, Oxford, 1966, pp. 111–144.

[17] Gutman, L. N., "Theoretical Model of a Waterspout," *Bulletin of the Academy of Sciences of the USSR* (Geophysical Series), Vol. 1, Pergamon Press translation, New York, 1957, pp. 87–103.

[18] Smith, R. K., "The Surface Boundary Layer of a Hurricane," *Tellus*, Vol. 20, Almquist and Wiksells Boktryckeri, Stockholm, 1968, pp. 473–484.